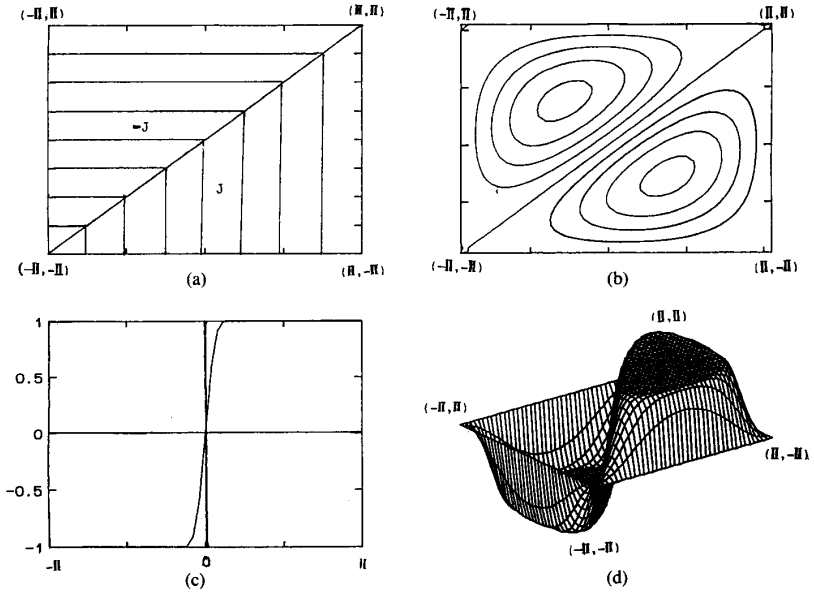

Fig. 1. (a) Ideal frequency response to be approximated. (b) Contours of the function ($F(w_1, w_2)$ appropriate to this problem. (c) 1-D prototype filter. (d) The frequency response to the resulting 2-D FIR filter designed by this transformation.

frequency response. Some other applications will be researched in the future.

References

[1] J. H. McClellan, "The design of two dimensional digital filters by transformation," in *Proc. 7th Ann. Princeton Conf. Information Sci.*, 1973, pp. 247-51.

[2] R. M. Mersereau, "The design of arbitrary 2-D zero-phase FIR filters using transformation," *IEEE Trans. Circuits Syst.*, vol. CAS-27, pp. 142-144, Feb. 1980.

[3] D. E. Dudgeon and R. M. Mersereau, *Multidimensional Digital Signal Processing*. Englewood Cliffs, NJ: Prentice-Hall, 1984.

[4] Y.-L. Tai and T.-P. Lin, "Design of Hilbert transformer by multiple use of the same filter," *Electron. Lett.*, vol. 25, no. 19, pp. 1288-1290, Sept. 1989.

[5] L. R. Rabiner and B. Gold, *Theory and Application of Digital Signal Processing*. Englewood Cliffs, NJ: Prentice-Hall, 1975.

[6] J. H. McClellan, T. W. Parks, and L. R. Rabiner, "A computer program for designing optimum FIR linear phase digital filters," *IEEE Trans. Audio Electroacoust.*, vol. AU-21, pp. 506-526, Dec. 1973.

[7] A. V. Oppenheim and R. W. Schafer, *Discrete Time Signal Processing*. Englewood Cliffs, NJ: Prentice-Hall, 1989.

Iterative Procedures for Reduction of Blocking Effects in Transform Image Coding

Avideh Zakhor

***Abstract*—We propose a new iterative block reduction technique based on the theory of projection onto convex sets. The basic idea behind this technique is to impose a number of constraints on the coded image in such a way as to restore it to its original artifact-free form. One such constraint can be derived by exploiting the fact that the transform-coded image suffering from blocking effects contains high-frequency vertical and horizontal artifacts corresponding to vertical and horizontal discontinuities across boundaries of neighboring blocks. Since these components are missing in the original uncoded image, or at least can be guaranteed to be missing from the original image prior to coding, one step of our iterative procedure consists of projecting the coded image onto the set of signals that are bandlimited in the horizontal or vertical directions. Another constraint we have chosen in the restoration process has to do with the quantization intervals of the transform coefficients. Specifically, the decision levels associated with transform coefficient quantizers can be used as lower and upper bounds on transform coefficients, which in turn define boundaries of the convex set for projection. Thus, in projecting the "out-of-bound" transform coefficient onto this convex set, we will choose the upper (lower) bound of the quantization interval if its value is greater (less) than the upper (lower) bound. We present a few examples of our proposed approach.**

Manuscript received June 10, 1991; revised February 3, 1992. This work has been supported by IBM, Eastman Kodak Company, TRW, and the National Science Foundation contract MIP-9057466. This paper was recommended by Associate Editor Dimintris Anastassiou.

The author is with the Department of Electrical Engineering and Computer Sciences, University of California, Berkeley, CA 94720.

IEEE Log Number 9107519.

I. Introduction

Transform coding is one of the most widely used image compression techniques. It is based on dividing an image into small blocks, taking the transform of each block and discarding high-frequency coefficients and quantizing low-frequency coefficients. Among various transforms, the discrete cosine transform (DCT) is one of the most popular because its performance for certain class of images is close to that of the Karhunen-Loeve transform (KLT), which is known to be optimal in the mean squared error sense.

Although DCT is used in most of today's standards such as JPEG and MPEG, its main drawback is what is usually referred to as the "blocking effect." Dividing the image into blocks prior to coding causes blocking effects—discontinuities between adjacent blocks—particularly at low bit rates. In this paper, we present an iterative technique for the reduction of blocking effects in coded images.

II. Iterative Restoration Method

The block diagram of our proposed iterative approach is shown in Fig. 1. The basic idea behind our technique is to impose a number

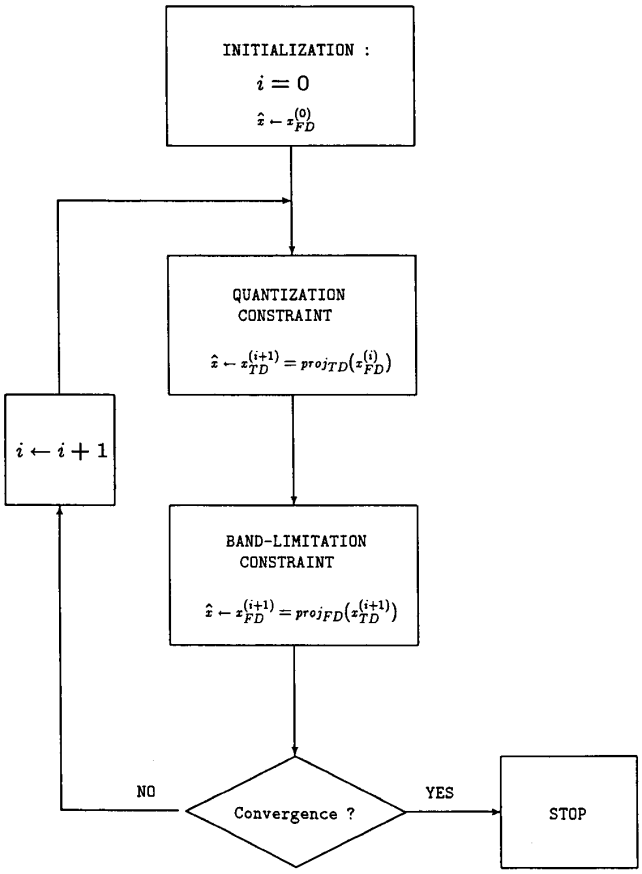

Fig. 1. Block diagram of the iterative algorithm.

of constraints on the coded image in such a way as to restore it to its original artifact-free-form. We derive one such constraint from the fact that the coded image with $N \times N$ blocks has high-frequency horizontal and vertical artifacts corresponding to the discontinuities at the edges of the $N \times N$ blocks. Therefore, one step of our procedure consists of bandlimiting the image in the horizontal and vertical directions. We refer to this constraint as the filtering constraint.

We derive the second constraint from the quantizer and thus refer to it as the quantization constraint. Because the quantization intervals for each DCT coefficient is assumed to be known in decoding a DCT encoded image, the quantization constraint ensures that in restoring images with blocking effects, DCT coefficients of $N \times N$ blocks remain in their original quantization interval.

If S_1 denotes the set of bandlimited images, and S_2 denotes the set of images whose $N \times N$ DCT coefficients lie in specific quantization intervals, our goal can be stated as that of finding an image in the intersection of S_1 and S_2. One way to achieve this is to start with an arbitrary element in either of the two sets and iteratively map it back and forth to the other set, until the process converges to an element in the intersection of the two sets. Under these conditions convergence can be guaranteed by the theory of projection onto convex sets (POCS) if sets S_1 and S_2 are convex, and if the mapping from each set to the other is a projection [6]. By definition, the projection of an element x in set A onto set B is equivalent to finding the closest element, according to some metric, in B to x.

To apply the above idea to our problem, we first notice that two sets S_1 and S_2 are both convex. We also choose the mean squared error as our metric of closeness. This implies that a projection from S_2 to S_1 can be accomplished by any bandlimitation algorithm such as ideal low-pass filtering. It also implies that projection from S_1 to S_2 can be accomplished by moving $N \times N$ DCT coefficients that are outside their designated quantization interval to the closest boundary of their respective quantization intervals. For instance, if a particular $N \times N$ DCT coefficient, which is supposed to be in the range $[a, b]$, takes on a value greater than b, it is projected to b. Alternatively, if it takes on a value smaller than a it is projected onto a.

Having explained the constraints, convex sets, and projections, we now summarize our proposed iterative procedure shown in Fig. 1. In the first part of each iteration, we low pass filter, or bandlimit, the image that has high-frequency horizontal and vertical components corresponding to the discontinuities between $N \times N$ blocks. In the second part of each iteration we apply the quantization constraint as follows. First we divide the image into $N \times N$ blocks and take the DCT of each. Then we project any coefficient outside its quantization range onto its appropriate value. Under these conditions, the POCS theory guarantees that iterative projection between the sets S_1 and S_2 results in convergence to an element in the intersection of the two sets.

III. Experimental Results

Fig. 2(a) shows the original, unquantized 512 × 512 Lena, and (b), (c), and (d) show its JPEG encoded version to 0.43, and 0.24,

(a)

(b)

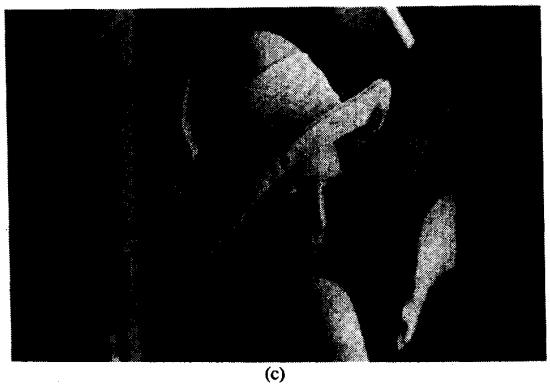

(c)

(d)

Fig. 2(a) Original 512 × 512 image, Lena. 2(b) Lena quantized to 0.43 bpp. 2(c) Lena quantized to 0.24 bpp. 2(d) Lena quantized to 0.15 bpp.

and 0.15 bpp, respectively. The quantization tables for Figs. 2(b), (c), and (d) are included in the Appendix.

Strictly speaking, the band-limitation portion of our algorithm corresponds to a true projection if the image under consideration is convolved with an ideal low-pass filter. Since an ideal low-pass filter cannot be implemented in practice, we have chosen to approximate it with a 3 × 3 finite impulse response (FIR) filter of the form

$$\begin{aligned} h(0,0) &= 0.2042, \\ h(0,1) &= h(0,-1) = h(1,0) = h(-1,0) = 0.1239 \\ h(0,2) &= h(0,-2) = h(2,0) = h(2,0) = 0.0751. \end{aligned} \quad (1)$$

We now show examples of our iterative algorithm. Fig. 3(a) shows five iterations of our algorithm applied to the 0.43-bpp quantized image of Fig. 2(b). The FIR filter of (1) was used for the band-limitation step. As Fig. 2(b) shows, blocking artifact has been removed without introducing excessive blurring. For comparison purposes, the result of applying the low-pass filter in (1) to Fig. 2(b) for five times, without applying the quantization constraint, is also shown in Fig. 3(b). Although consecutive low-pass filtering removes most of the blocking effect, it blurs the image in a noticeable way. We have found that applying the low-pass filter of (1) once rather than five times, results in a less blurry image than in Fig. 3(b), but at the same time does not remove all the blocking effect.

Figs. 4(a) and (b) show application of our algorithm to the 0.24-bpp quantized image of Fig. 2(c) for 5 and 20 iterations, respectively. The FIR filter of (1) was used for the band-limitation step. As seen, the blocking artifact is better removed in Fig. 4(b) than in 4(a), while they are as sharp as each other. For comparison purposes, Fig. 4(c) and (d) show the result of applying the low-pass filter of (1) to Fig. 2(c), 5 and 20 times, respectively. Comparing Fig. 4(c) and 4(d) to Fig. 4(a) and (b), respectively, we find that the latter pair are more blurry than the former. Thus, applying the quantization constraint prevents the images from becoming excessively blurry.

Fig. 5(a) shows application of our algorithm to the 0.15-bpp quantized image of Fig. 2(d) for 20 iterations. The FIR filter of (1) was used for the band-limitation step. For comparison purposes, Fig. 5(b) shows the result of applying the low-pass filter of (1) to Fig. 2(d), 20 times. Comparing Fig. 5(b) to 5(a), we find that the latter is considerably more blurry than the former.

IV. Conclusions

The major conclusions to be drawn from this paper are as follows: 1) the proposed iterative algorithm using a 3 × 3 low-pass filtering of (1) results in images that are free of blocking artifacts and excessive blurring; 2) low-pass filtering by itself could remove blockiness but at the expense of increased blurriness.

It is conceivable to generate images similar to Figs. 5(a) and 4(b) without having to apply our algorithm for as many as 20 iterations. Our conjecture is that this could be achieved by increasing the region of support of the impulse response of the filter of (1). In practical hardware implementations however, 3 × 3 convolvers are more readily available than, say, 30 × 30 ones.

We have checked the convergence of our algorithm and found that it converges after 20 iterations or so. This is encouraging since there is no guarantee that the intersections of our particular convex sets is nonempty, and the theory of POCS only guarantees convergence in situations where the intersection is nonempty.

One way to increase the likelihood of convergence is to vary the confidence with which the ideal solution is in the chosen constraint set, by varying its size. For example, if we choose prototype constraint sets as in [10], using the statistics of the

(a)

(b)

Fig. 3(a) Result of applying the iterative algorithm to Fig. 2(b) for five iterations with the low-pass filter of (1) used for bandlimitation. (b) Result of low-pass filtering Fig. 2(b) five times using the filter in (1).

quantization noise, we can change the boundaries and the size of the constraint set in a controlled fashion and therefore increase the likelihood of a solution in the intersection of the constraint sets. Examples of such prototype constraint sets include bounded variation from the Weiner solution and pointwise adaptive smoothness. The latter constraint has the obvious advantage of being locally adaptive to changes in the characteristics of the image. Projection onto fuzzy sets is another way of increasing the size of our convex sets [9].

APPENDIX

The quantization table for Fig. 2(b) is

20	24	28	32	36	80	98	144
24	24	28	34	52	70	128	184
28	28	32	48	74	114	156	190
32	34	48	58	112	128	174	196
36	52	74	112	136	162	206	224
80	70	114	128	162	208	242	200
98	128	156	174	206	242	240	206
144	184	190	196	224	200	206	208

For Fig. 2(c) it is

50	60	70	70	90	120	255	255
60	60	70	96	130	255	255	255
70	70	80	120	200	255	255	255
70	96	120	145	255	255	255	255

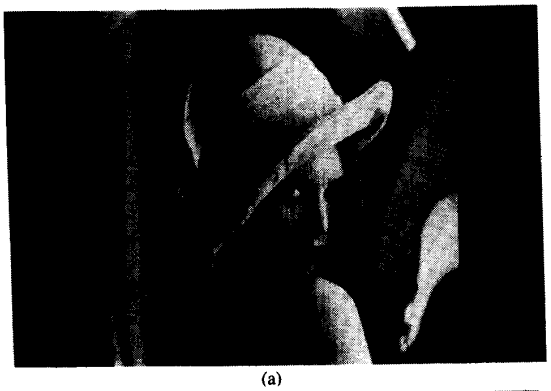

(a)

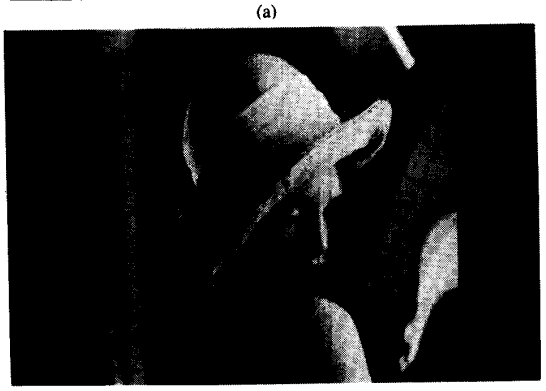

(b)

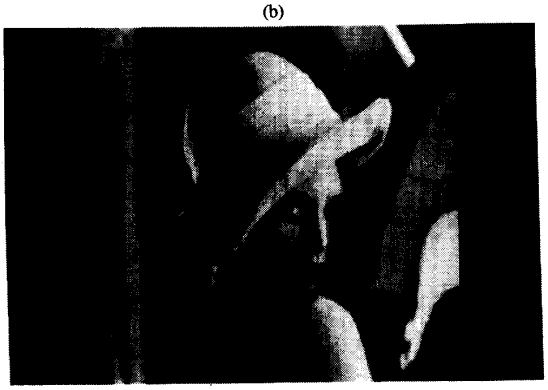

(c)

(d)

Fig. 4(a) Result of applying the iterative algorithm to Fig. 2(c) for 5 iterations with the low-pass filter of (1) used for bandlimitation. (b) Result of applying the iterative algorithm to Fig. 2(c) for 20 iterations with the low-pass filter of (1) used for bandlimitation. (c) Result of low-pass filtering Fig. 2(c) five times using the filter in (1). (d) Result of low-pass filtering Fig. 2(c) 20 times using the filter in (1).

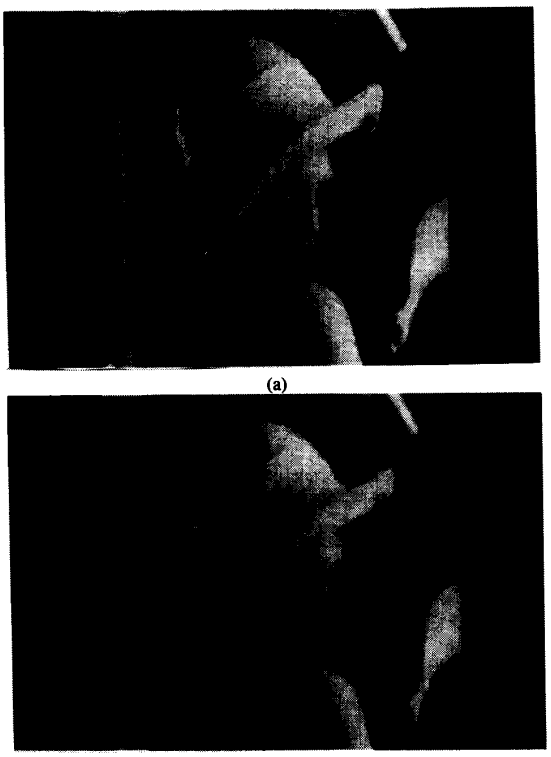

(a) (b)

Fig. 5(a) Result of applying the iterative algorithm to Fig. 2(d) for 20 iterations with the low-pass filter of (1) used for bandlimitation. (b) Result of low pass filtering Fig. 2(d) 20 times using the filter in (1).

90	130	200	255	255	255	255	255
120	255	255	255	255	255	255	255
255	255	255	255	255	255	255	255
255	255	255	255	255	255	255	255

and for Fig. 2(d) it is:

110	130	150	192	255	255	255	255
130	150	192	255	255	255	255	255
150	192	255	255	255	255	255	255
192	255	255	255	255	255	255	255
255	255	255	255	255	255	255	255
255	255	255	255	255	255	255	255
255	255	255	255	255	255	255	255
255	255	255	255	255	255	255	255

The 255 entry in the above tables indicates that the coefficient was discarded.

References

[1] H. C. Reeve and J. S. Lim, "Reduction of blocking effects in image coding," *Optical Eng.*, vol. 23, no. 1, pp. 34-37, Jan./Feb. 1984.

[2] J. Biemond, R. L. Lagendijk, and R. M. Mersereau, "Iterative methods for image deblurring," *Proc. IEEE*, vol. 78, no. 5, pp. 856-883, May 1990.

[3] S. N. Efstratiadis and A. K. Katsaggelos, "Adaptive iterative image restoration with reduced computational load," *Optical Eng.*, vol. 29, no. 12, pp. 1458-1468, Dec. 1990.

[4] S. J. Reeves and R. M. Mersereau, "Optimal estimation of the regularization parameter and stabilizing functional for regularized image restoration," *Opt. Eng.*, vol. 29, no. 5, pp. 446-454, May 1990.

[5] B. J. Sullivan and A. K. Katsaggelos, "New termination rule for linear iterative image restoration algorithms," *Opt. Eng.*, vol. 29 no. 5, pp. 471-477, May 1990.

[6] D. C. Youla and H. Webb, "Image restoration by the method of convex projections: Part 1—Theory," *IEEE Trans. Med. Imag.* vol. 1, no. 2, pp. 81-94, Oct. 1982.

[7] A. Zakhor and A. V. Oppenheim, "Reconstruction of two-dimensional signals from level crossings," *Proc. IEEE*, vol. 78, no. 1, pp. 31-55, Jan. 1990.

[8] A. Abo-Taleb and M. M. Fahmy, "Design of FIR two-dimensional digital filters by successive projections," *IEEE Trans. Circuits Syst.*, vol. CAS-31, no. 9, pp. 801-805, Sept. 1984.

[9] M. R. Civanlar and H. J. Trussell, "Digital image restoration using fuzzy sets," *IEEE Trans. Acoust. Speech, Signal Processing*, vol. 34, pp. 919-936, 1986.

[10] "Set-theoretic image restoration," *IEEE Trans. Signal Processing*," *vol.* 39, *no.* 10, *pp.* 2275-2285, *Oct.* 1991.

Comments on "Interpolative Multiresolution Coding of Advanced Television with Compatible Subchannels"

T. Naveen and John W. Woods

I. Introduction

Recently, Uz *et al.* [1] have analyzed the propagation of quantization noise in a pyramid (with feedback) and subband decomposition schemes. In this study each band was independently quantized by a scalar quantizer of equal step size. The resulting reconstruction error spectrum indicated that in both the pyramid (without feedback) and subband coding schemes, noise was building up in lower frequencies (see their Fig. 6). They have indicated two possible solutions to this problem: use a pyramid with feedback or choose finer quantizers for the lower bands. The latter solution has been known to the researchers. This solution can be explained from the rate-distortion theoretic point of view, as given in Section II. This solution has been implicitly provided in [2].

II. Rate Allocation Problem

In this section, we review the analysis given in [2](Section 1.3) for bit allocation to subbands when PCM coding is used. Let us consider a code rate of R bits/sample (bps), and an N sample image source analyzed into M subbands with n_m samples in mth subband so that

$$N = \sum_{m=1}^{M} n_m. \tag{1}$$

The distortion-rate characteristic (MSE) of a scalar quantizer for a unit variance sample can be modeled as

$$\rho(r) = g(r)e^{-ar} \qquad r \geq 0 \tag{2}$$

for $g(r)$ a slowly varying algebraic function of rate per sample r and a a constant no greater than $2\log_e 2$. For simplicity, let us assume that $g(r) \triangleq g$, a constant. Let a rate of r_m bps be used to

Manuscript received July 25, 1991 and January 9, 1992. This work was supported in part by National Science Foundation grant NCR-9003754.

The authors are with the Electrical, Computer, and Systems Engineering Department, Rensselaer Polytechnic Institute, Troy, NY 12180-3590.

IEEE Log Number 9107419.